ISBN: 978-3-95450-223-3 ISSN: 2673-7000 doi:10.18429/JACoW-NAPAC2019-WEPLE04

RECENT DEVELOPMENTS AND APPLICATIONS OF PARALLEL MULTI-PHYSICS ACCELERATOR MODELING SUITE ACE3P*

Z. Li #, L. Ge, C.-K. Ng, L. Xiao, SLAC, Menlo Park, CA, USA

Abstract

SLAC's ACE3P code suite is developed to harness the power of massively parallel computers to tackle large complex problems with increased memory and solve them at greater speed. ACE3P parallel multi-physics codes are based on higher-order finite elements for superior geometry fidelity and better solution accuracy. ACE3P consists of an integrated set of electromagnetic, thermal and mechanical solvers for accelerator modeling and virtual prototyping. The use of ACE3P has contributed to the design and optimization of existing and future accelerator projects around the world. Multi-physics analysis on high performance computing (HPC) platform enables thermal-mechanical simulations of largescale systems such as the LCLS-II cryomodule. Recently, new capabilities have been added to ACE3P including a nonlinear eigenvalue solver for calculating mode damping, a moving window for pulse propagation in the time domain to reduce computational cost, thin layer coating representation using a surface impedance model, and improved boundary conditions using perfectly matched layers (PML) to terminate wave propagation. These new developments are presented in this paper.

INTRODUCTION

High performance computing (HPC) for accelerator modeling and simulation has played an important role in the design and optimization of existing and future accelerators. Next generation x-ray free electron laser light source and ultra-fast electron diffraction/microscopy (UED/UEM) put stringent requirements for high electron beam quality. In order to design and to optimize accelerators to generate such high brightness beams, high-fidelity simulations that include both self-consistent charged particle interactions and RF fields of beamline components with realistic geometry details are needed.

ACE3P is a parallel finite element electromagnetics modeling suite developed for accelerator cavity and structure design including integrated multiphysics effects. While ACE3P is implemented on various parallel computing platforms, the unique advantage of ACE3P is its massively parallel capability running on supercomputers accessible to thousands of processors. With optimized scalability on high performance computing facilities, the multi-physics solvers of ACE3P are capable of handling large problem size with realistic details to achieve numerical prototyping analysis of RF, field emission, multipacting, and thermal/structural of the RF systems, leading to time and cost saving for accelerator development. The use of ACE3P has contributed to the design and optimization of existing and future accelerator projects around the world, such as the ILC, LHC, LCLS-I/II and high gradient accelerators. Reliable 3D accelerator structure models produced using the ACE3P solvers are being directly applied for engineering designs.

The code dissemination has been carried out via Code Workshops [1] and user support by the ACE3P development team. Over the years, new solvers and features have been added to existing capabilities to meet the demands of ever-growing comprehensive modeling needs. In addition, code integration of ACE3P with other high-performance beam dynamics and plasma codes are being carried out to provide a unique HPC capability on supercomputers to address critical accelerator design and operation issues including RF, beam breakup, beam quality and machine protection.

ACE3P CODE SUITE

Six simulation modules have been developed in ACE3P to address different physics aspects of accelerator applications [2-4]. The modeling capabilities of each ACE3P module are summarized as follows.

Omega3P: a complex eigensolver for finding normal modes in resonant structures with open ports, impedance boundaries or lossy materials;

S3P: a frequency domain solver for calculating scattering parameters of RF components;

T3P: a time-domain solver for simulating transient response of RF driven systems and for calculating wakefields due to charged beams;

Track3P: a particle tracking code for calculating dark current and analyzing multipacting in RF cavities and components;

Pic3P: a particle-in-cell code for self-consistent simulation of particle and RF field interactions in RF guns and klystrons;

TEM3P: an integrated multi-physics code including electromagnetic/thermal/mechanical effects for cavity design.

The 3D solid model and meshing is handled by the geometry and meshing tool CUBIT [5] developed at Sandia National Lab. Physics parameters of the solver data are analyzed using the postprocessing tool ACDTool and visualized using Paraview [6].

New solver and features have recently been added to the ACE3P capabilities that include the non-linear eigensolver, perfect boundary layer model, surface impedance model, and ongoing integration with beam dynamics codes IMPACT [7] and WARP [8]. These new implementations are described in the following sections.

*Work supported by the US Department of Energy under contract DE-AC02-76SF00515.
#lizh@slac.stanford.edu

ISBN: 978-3-95450-223-3 ISSN: 2673-7000 doi:10.18429/JACoW-NAPAC2019-WEPLE04

NON-LINEAR ENGENSOLVER

The eigenvalue problem for solving the Maxwell equation is represented by

$$\nabla \times \left(\frac{1}{\mu}\nabla \times \vec{E}\right) - \epsilon k^2 \vec{E} = 0 \quad (1)$$

with boundary conditions for perfect conductor or electric and magnetic symmetry planes

$$\vec{n} \times \vec{E} = 0, \quad on\ \Gamma_E$$
$$\vec{n} \times (\vec{n} \times \vec{E}) = 0, \quad on\ \Gamma_M$$

and for the boundaries at the ports

$$\vec{n} \times \left(\frac{1}{\mu}\vec{n} \times \vec{E}\right) - i\gamma_0 e_0^{TEM} \int_\Gamma e_0^{TEM} \cdot \vec{E} d\Gamma - i\sum_m \gamma_m e_m^{TM} \int_{\Gamma_m} e_m^{TM} \cdot \vec{E} d\Gamma_m + i\sum_m \frac{k^2}{\gamma_m} e_m^{TE} \int_{\Gamma_m} e_m^{TE} \cdot \vec{E} d\Gamma_m = 0$$

where $\gamma_0 = \sqrt{k}$ and $\gamma_m = \sqrt{k^2 - (k_m^c)^2}$, with $k_m^c = 2\pi f_m^c$ being the cutoff wavenumber of the mth waveguide mode. The normalized waveguide transverse electric and magnetic (TEM) mode, the mth transverse electric (TE) mode, and the mth transverse magnetic (TM) mode, onto the waveguide boundaries are given by e_0^{TEM}, e_m^{TE}, and e_m^{TM}, respectively.

By representing the electric field in terms of hierarchical higher-order Nedelec basis functions $\vec{N}$ [9],

$$\vec{E} = \sum_i x_i \vec{N}_i$$

together with the multi-port-mode boundary conditions, the discretized Maxwell equation becomes a non-linear eigenvalue problem:

$$F(\lambda)x = 0 \quad (2)$$

with

$$F(\lambda) = K - \lambda M + i\sqrt{\lambda} W^{TEM} + i\sum_m \sqrt{\lambda - k_m}\, W_m^{TE} + i\sum_m \frac{\lambda}{\sqrt{\lambda - k_m}} W_m^{TM}$$

where K and M are the stiff and mass matrices, $W_m^{TEM,TE,TM}$ are matrices related to the waveguide ports. The non-linear problem (2) is generally hard to solve. Recently, we have collaborated with LBNL and developed a non-linear eigenvalue solver to address this type of problems [10]. The solution of the non-linear eigensolver relies on using a rational approximation to the nonlinear terms by reducing the equation to a rational eigenvalue problem. A special linearization procedure turns the rational eigenvalue problem into a larger linear eigenvalue problem that can be solved by existing iterative methods. The solving procedure is composed of three steps: (i) approximation of the scalar nonlinear functions by interpolating rational functions, yielding a rational eigenvalue problem; (ii) linearization of the resulting rational eigenvalue problem, i.e., a reformulation of the rational eigenvalue problem as a generalized (linear) eigenvalue problem with the same eigenvalues but much larger in problem size; (iii) solving the generalized eigenvalue problem by a CORK (compact rational Krylov) method.

The non-linear eigensolver was applied to obtain the Qext of the 3rd dipole band modes of a LCLS-II superconducting cryomodule and compared with the experimental results. The 3rd dipole band modes have frequencies around 2.5 GHz which are above the beampipe cutoff frequency of 2.253 GHz. The presence of propagating modes of different cutoff frequencies at the coupler ports (FPC and HOM) and the beam pipes (see Fig. 1) makes the problem nonlinear. Previously, in order to establish a solvable eigen system, one has to apply approximate boundary conditions at the beampipe boundary, e.g. perfect E/B or simple absorbing conditions, which introduced errors in the Qext calculation. The nonlinear eigensolver mades it possible to ensure exact termination of waveguide modes at the ports. The simulation model includes 8 cavities of the cryomodule. The couplers and the end beam pipes are all treated as matched waveguides. The lowest cutoff mode in the couplers is a TEM mode while at the beam pipe is a TE11 mode. The E field contour plot of a 3rd band dipole mode in Fig. 1 shows propagation of the fields in the end beam pipes, indicating a port boundary treatment at the beam pipes is necessary. Both the calculated and measured Qext of the 3rd band dipole are plotted in Fig. 2 for comparison and are in good agreement.

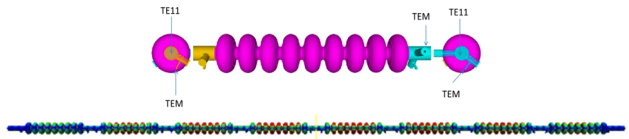

Figure 1: (top) 9-cell cavity with couplers; (bottom) Electric field contour plot of a 3rd dipole band mode in the LCLS-II 8-cavity cryomodule.

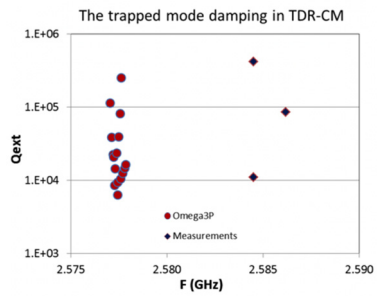

Figure 2: Qext of the 3rd dipole band modes in the LCLS-II cryomodule calculated using the CORK nonlinear eigensolver and their comparison with measurements.

SURFACE IMPEDANCE MODEL

A thin layer of coating material on a conducting surface such as a thin rain film on a transmission line can have significant effects on RF wave propagation. Typically, the thickness of the layer is orders of magnitude smaller than the overall simulation domain. Modeling with a physically meshed layer may lead to a prohibitively large overall problem size. Without losing much accuracy, such a thin layer can be modeled effectively using a mathematical

ISBN: 978-3-95450-223-3 ISSN: 2673-7000 doi:10.18429/JACoW-NAPAC2019-WEPLE04

model without needing of a physical volume mesh in the layer. We have implemented a surface impedance boundary condition (SIBC) in the time domain solver T3P using the mathematical model described in [11] for a dielectric layer on a conductor. Using the SIBC to represent the dielectric coating on conductor greatly eases the mesh generation and reduces computational requirements. The SIBC treatment of the thin layer is validated using a simple model as shown in Fig. 3. This model is consisted of a 1-meter long coax cable with a half meter in the middle coated with a 1 mm thick dielectric material on the inner conductor. The coated material has a dielectric constant of 74 and an electrical conductivity of 5 S/m at 5 GHz. This model is simulated using the SIBC model as well as with a physical mesh layer. Good agreement was obtained between the two simulations as shown in Fig. 3.

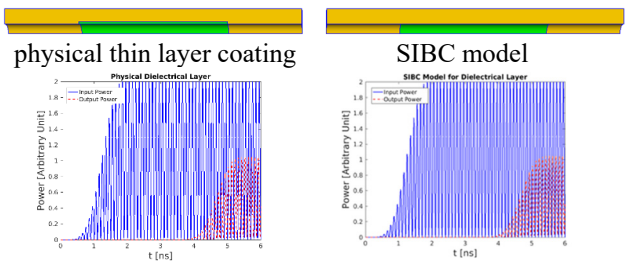

Figure 3: The power at input and output ports from physical dielectric layer (left) and SIBC model (right).

PML FOR FREE SPACE TERMINATION

To improve the termination of broadband RF pulse propagation, a new boundary condition using perfectly matched layers (PML) to terminate wave propagation has been implemented in the time domain solver T3P. The formulation is based on the work described in [12]. The computational domain is terminated by rectangular blocks in x, y and z directions represented by artificial conductivities. Implementation in all spatial directions can model wave absorption in free space, which will be more accurate than the current absorbing boundary condition (ABC) in T3P for absorbing electromagnetic radiation such as from photonic fibers used in dielectric laser acceleration [13]. The PML can also be applied for termination of wave propagation in waveguides to absorb broad-band signals. As an example, we excite an electric dipole at the center of a cubic volume with PML added in all directions. Figure 4 shows the signal monitored at a location near the edge of the cubic volume. The result shows only outgoing pulse without reflection by the boundary, indicating total absorption of the RF pulse by the PML.

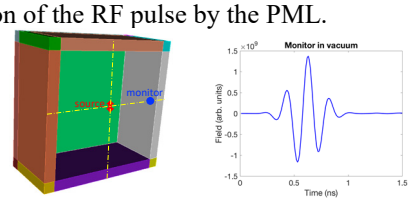

Figure 4: (left) A simple model for benchmarking the PML implemented in T3P. (right) A dipole source excites a short pulse at the center of the volume. The monitored signal showed the outgoing pulse and no reflection by the PML.

LARGE SCALE MULTI-PHYSICS MODELING

Large scale thermal-mechanical analysis can be performed using the multi-physics solvers of the ACE3P. One application is the calculation of the LCLS-II cryomodule distortion due to thermal effects. The temperature gradient in the tunnel (ground to ceiling) and the RF heating of the FPC couplers could cause a bowing distortion along the cryomodule. This bowing can cause shift in the antenna position of the FPC couplers resulting in an RF coupling deviation in the cavities. It is important to quantify these effects under realistic tunnel conditions. The TEM3P multi-physics solver was used to simulate the LCLS-II cryomodule with the thermal boundary conditions of the LCLS-II tunnel. The results are shown in Figs. 5 and 6. The deviation of FPC coupling was estimated to confirm the margin needed in RF power to compensate this effect.

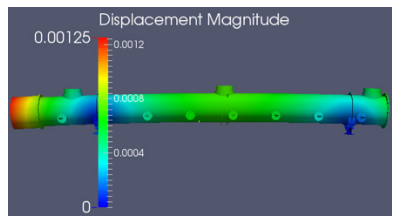

Figure 5: The displacement distribution on the vacuum vessel due to a ground-ceiling temperature gradient in the accelerator tunnel (deformation scaled by 100 for visualization).

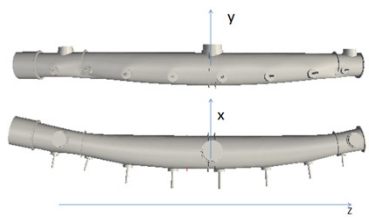

Figure 6: The amplified deformed vacuum vessel caused by the FPC RF heating in the warm section (scaled by 500 for visualization).

ONGOING DEVELOPMENT

Ongoing development of ACE3P includes the code integration with beam dynamics and plasma simulations codes IMPACT and WARP. The integration takes advantage of high fidelity RF fields of the ACE3P solvers and parallel tracking and comprehensive physics models of particles of IMPACT and WARP. Initial benchmark simulations have been performed on the LCLS-II injector beam dynamics [14] and LCLS-II cavity plasma cleaning [15]. Details of the code integration is presented in [16] and [17]. The goal is to produce a unique high-performance modelling toolset that can address the broad accelerator design challenges for future high energy accelerators and light sources.

REFERENCES

[1] https://conf.slac.stanford.edu/cw18/

ISBN: 978-3-95450-223-3 ISSN: 2673-7000 doi:10.18429/JACoW-NAPAC2019-WEPLE04

[2] C.-K. Ng *et al.*, "Advances in Parallel Finite Element Code Suite ACE3P," in *Proc. 6th Int. Particle Accelerator Conf. (IPAC'15)*, Richmond, VA, USA, May 2015, pp. 702-704. doi:10.18429/JACoW-IPAC2015-MOPMN002

[3] K. Ko and A. E. Candel, "Advances in Parallel Electromagnetic Codes for Accelerator Science and Development," in *Proc. 25th Linear Accelerator Conf. (LINAC'10)*, Tsukuba, Japan, Sep. 2010, paper FR101, pp. 1028-1032.

[4] O. Kononenko *et al.*, "3D Multiphysics Modeling of Superconducting Cavities with a Massively Parallel Simulation Suite," *Phys. Rev. Accel. Beams*, vol. 20, p. 102001, 2017.

[5] https://cubit.sandia.gov/

[6] https://www.paraview.org/

[7] http://blast.lbl.gov/blast-codes-impact/

[8] https://blast.lbl.gov/blast-codes-warp/

[9] D. Sun, J. Lee, and Z. Cendes, "Construction of nearly orthogonal Nedelec bases for rapid convergence with multilevel preconditioned Solvers," *SIAM Journal on Scientific Computing*, vol. 23, p. 1053, 2001. doi:10.1137/S1064827500367531

[10] R. Van Beeumen *et al.*, "Computing resonant modes of accelerator cavities by solving nonlinear eigenvalue problems via rational approximation," *J. Computational Physics*, vol. 374, p. 1031, Dec. 2018. https://doi.org/10.1016/j.jcp.2018.08.017

[11] G. Kobidze *et al.*, "Implementation of Collocated Surface Impedance Boundary Conditions in FDTD," *IEEE Trans. on Antennas and Propagation*, vol. 58, no. 7, July 2010. doi:10.1109/TAP.2010.2048859

[12] J.-M. Jin, D.J. Riley, *Finite Element Analysis of Antennas and Arrays*, John Wiley & Sons, Inc., 2009.

[13] C.-K. Ng *et al.*, "Transmission and Radiation of an Accelerating Mode in a Photonic Bandgap Fiber," SLAC-PUB-14156.

[14] J. Qiang, D. A, L. Ge, Z. Li, C.-K. Ng, and L. Xiao, "Integration of Cavity Design and Beam Dynamics Simulation Using the Parallel IMPACT and the ACE3P Codes", in *Proc. 10th Int. Particle Accelerator Conf. (IPAC'19)*, Melbourne, Australia, May 2019, pp. 3317-3320. doi:10.18429/JACoW-IPAC2019-WEPTS088

[15] M. Martinello *et al.*, "Plasma Processing R&D for LCLS-II Cavities," presented at *IPAC'2017*, Copenhagen, Denmark, May 2017, slides THOBB2.

[16] L. Ge *et al.*, "Integrated Accelerator Simulation with Electromagnetics and Beam Physics Codes," presented at NAPAC'19, Lansing, Michigan, USA, Sept. 2019, paper WEPLE02, this conference.

[17] D. Bizzozero *et al.*, "Simulation Analysis of the LCLS-II Injector Using ACE3P and IMPACT," presented at NAPAC'19, Lansing, Michigan, USA, Sept. 2019, paper WEPLS05, this conference.